Dose-dependent Neuroprotection of $VEGF_{165}$ in Huntington's Disease Striatum

Stuart M Ellison[1], Antonio Trabalza[1], Veronica Tisato[1,2], Evangelos Pazarentzos[1,3], Shirley Lee[1], Vasiliki Papadaki[1], Despoina Goniotaki[1], Sarah Morgan[1], Nazanin Mirzaei[1] and Nicholas D Mazarakis[1]

[1]Division of Brain Sciences, Department of Gene Therapy, Faculty of Medicine, Centre for Neuroinflammation & Neurodegeneration, Imperial College London, Hammersmith Hospital Campus, London, UK; Current Addresses: [2]Department of Morphology and Embryology and LTTA Centre, University of Ferrara, Ferrara, Italy; [3]Division of Hematology/Oncology, Helen Diller Comprehensive Cancer Center, University of California, San Francisco, California, USA

Huntington's disease (HD) is a devastating neurodegenerative disorder caused by abnormal polyglutamine expansion in the huntingtin protein (Exp-Htt). Currently, there are no effective treatments for HD. We used bidirectional lentiviral transfer vectors to generate *in vitro* and *in vivo* models of HD and to test the therapeutic potential of vascular endothelial growth factor 165 ($VEGF_{165}$). Lentiviral-mediated expression of Exp-Htt caused cell death and aggregate formation in human neuroblastoma SH-SY5Y and rat primary striatal cultures. Lentiviral-mediated $VEGF_{165}$ expression was found to be neuroprotective in both of these models. Unilateral stereotaxic vector delivery of Exp-Htt vector in adult rat striatum led to progressive inclusion formation and striatal neuron loss at 10 weeks post-transduction. Coinjection of a lower dose $VEGF_{165}$ significantly attenuated DARPP-32^+ neuronal loss, enhanced NeuN staining and reduced Exp-Htt aggregation. A tenfold higher dose $VEGF_{165}$ led to overt neuronal toxicity marked by tissue damage, neovascularization, extensive astrogliosis, vascular leakage, chronic inflammation and distal neuronal loss. No overt behavioral phenotype was observed in these animals. Expression of $VEGF_{165}$ at this higher dose in the brain of wild-type rats led to early mortality with global neuronal loss. This report raises important safety concerns about unregulated $VEGF_{165}$ CNS applications.

Received 19 February 2013; accepted 20 May 2013; advance online publication 25 June 2013. doi:10.1038/mt.2013.132

INTRODUCTION

Huntington's Disease (HD) is an autosomal dominant, fatal and progressive neurodegenerative genetic disease. The abnormality/mutation identified in 1993 is an expansion of the trinucleotide CAG repeat (>36 glutamines) 17 codons downstream of the initiation codon of the Huntingtin gene (*Htt*).[1] Patients with HD experience symptoms including chorea, involuntary muscle movements, cognitive impairment, personality, and behavioral changes at around 45–60 years of age. Death usually occurs 10–15 years following symptom onset. The expanded polyglutamine tract causes a toxic gain-of-function of the *Htt* gene, leading to death and dysfunction of the GABAergic medium spiny striatal neurons, which are the main neurons involved in early stage HD pathogenesis.[2] Abnormal polyglutamine aggregates, dysregulated transcription, disturbances of the proteolysis and proteosome protein degradation pathways, blockages of synaptic transmission, excitotoxicity, and mitochondrial disfunction have all been implicated in the neuronal pathology observed in HD (reviewed in ref. 3).

Currently there is no cure for HD and only symptomatic treatments are available. Research into anti-aggregating, autophagic, neurotrophic and gene knockdown therapeutic approaches is being pursued in HD. Molecular chaperones or heat shock proteins belong to a large family of proteins classified according to cellular localization, function and molecular weight.[4] These proteins are induced in times of stress and are responsible for refolding misfolded protein, regulation of protein quality control, fusion of vesicles, signal transmission processes, apoptosis, and proteosomal degradation.[4] Studies based on *C. elegans*, *Drosophila melanogaster*, *S.cerevisiae*, and rodent HD models have all illustrated the capability of these chaperones to suppress aggregate formation.[5–9] Neurotrophic factors, some downregulated by the transcriptional dysregulation in HD striatal neurons, such as brain-derived neurotrophic factor, glial-derived neurotrophic factor, and ciliary neurotrophic factor have been found to be neuroprotective in a variety of animal models of HD.[10–14]

Initially discovered in 1983 and cloned in 1989, vascular endothelial growth factor A (VEGF-A) is a multifunctional cytokine that exerts a variety of effects on vascular endothelial cells by interaction with receptors VEGFR1 and VEGFR2, that together promote the formation of new blood vessels.[15,16] Thus, in addition to rendering microvessels hyperpermeable, VEGF-A (including VEGF189, 165a and b and 121 forms mainly) stimulates endothelial cells to migrate and divide, profoundly altering their pattern of gene expression, and protecting them from apoptosis and senescence (reviewed in ref. 17).

As knockout of VEGF causes mouse embryonic lethality, transgenic mice with an altered VEGF gene (VEGF δ/δ) were created in which the hypoxia response element, located in the

Correspondence: *Nicholas D Mazarakis, Division of Brain Sciences, Department of Gene Therapy, Faculty of Medicine, Centre for Neuroinflammation & Neurodegeneration, Imperial College London, Hammersmith Hospital Campus, Burlington Danes Building, Du Cane Road, London W12 0NN, UK. E-mail: n.mazarakis@imperial.ac.uk*

VEGF gene promoter, was deleted. This enabled a reduction in VEGF expression in response to hypoxia while still allowing survival into adulthood. In these mice a delayed pathological phenotype resembling human amyotrophic lateral sclerosis (ALS) was observed.[18] This selective spinal motor neuron death was attributed to a diminished perfusion from blood vessels. Supplying VEGF$_{165}$ via retrogradely transported lentiviral vectors (LVs) to spinal motor neurons of the SOD1^{G93A} mouse model of ALS resulted in significant amelioration of disease phenotype.[19] These results confirmed the neurotrophic role of VEGF for motor neurons as subsequently substantiated by others.[20,21]

Lentiviruses are widely used and acknowledged as a powerful tool in gene therapy studies due to valuable characteristics such as; their ability to transduce both dividing and non-dividing cells, large insertion capacity (8–10 kb), long-term and stable expression of the inserted transgene, and minimal induction of immune

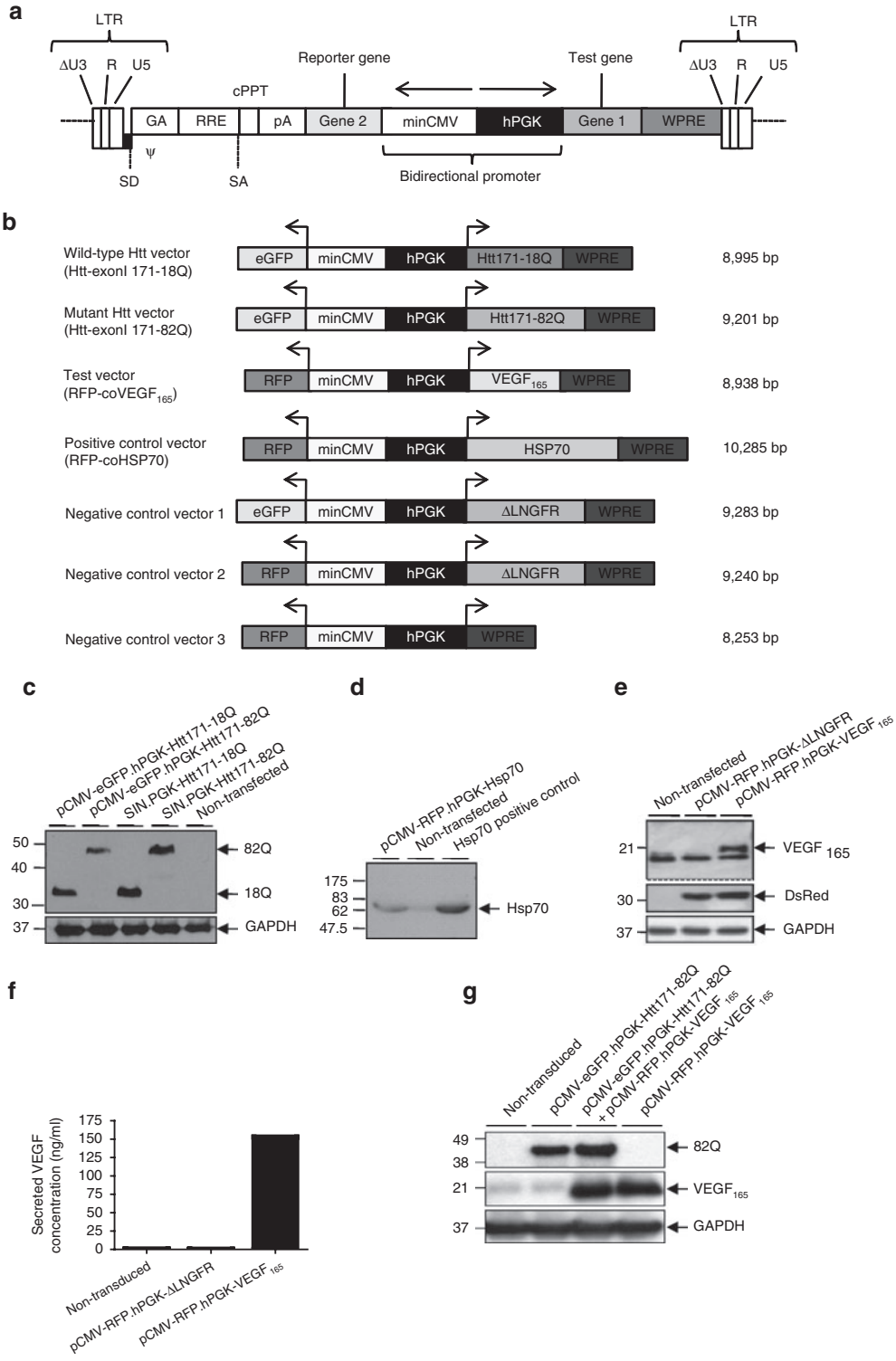

responses.[22] More importantly, recombinant LVs can be used to simulate disease states in animals. Specifically for HD, de Almeida *et al.* and Palfi *et al.* have used LVs encoding the mutant Htt fragments to induce the disease state in targeted striatal regions of the brain of rodents and primates and also established models of HD in primary neuronal cultures.[23–25] Perrin *et al.* and more recently Martin *et al.* demonstrated that lentiviral-mediated expression of Hsp104/Hsp27 or stress activated kinase MSK-1 can attenuate striatal dysfunction in these HD disease models.[6,26]

To investigate the possible neuroprotective effect of long-term VEGF-A expression in models of polyQ toxicity, we designed novel bidirectional vectors capable of both inducing *in vitro* and *in vivo* models of HD and transducing in specific therapeutic genes. Here, we report that VEGF$_{165}$ neuroprotects striatal neurons in these models but its effect is strictly dose dependent with higher doses inducing CNS neurodegeneration and neuroinfammation via pleiotropic vascular effects.

RESULTS

Design and expression of lentiviral transfer plasmids

So as to be able to trigger Htt-induced aggregate formation and neurodegeneration *in vitro* and *in vivo*, we cloned 18Q or 82Q and coexpressed with enhanced green fluorescent protein (eGFP) in bidirectional LVs based on a previously published vector system[27] (**Figure 1b**). We also cloned similar vectors to test VEGF$_{165}$ and Hsp70, which is known to be capable of ameliorating polyQ toxicity, and coexpressed them with red fluorescent protein (RFP).[6,8] By using the bidirectional lentivector systems and distinct marker genes (**Figure 1a**), we could spatially distinguish transduction with different vectors. Western blot analysis demonstrated that wild-type and Exp-Htt fragments (18Q and 82Q) and full-length human proteins for VEGF$_{165}$ or Hsp70 of the predicted molecular weight were expressed from these vectors (**Figure 1c–e**). As VEGF$_{165}$ is secreted, a specific ELISA confirmed its presence in supernatants of 293T cells transduced with VEGF$_{165}$ expressing LVs (**Figure 1f**). High level expression of the marker gene from these vectors was further detected by FACS or fluorescent microscopy following either transfection or transduction of 293T cells (data not shown). To evaluate if VEGF$_{165}$ affects Exp-Htt expression (82Q), 293T cells were cotransduced with both 82Q and VEGF$_{165}$ expressing LVs. Western blot analysis confirmed that there was no alteration in Exp-Htt expression in the cotransduced cells (**Figure 1g**).

VEGF$_{165}$ and Hsp70 are anti-aggregating in an 82Q SH-SY5Y model

We used human neuroblastoma SH-SY5Y cells, a neuronal cell line that exhibits moderate levels of dopamine beta hydroxylase activity and displays neuronal (MAP2$^+$) characteristics (data not shown), which have been used previously to generate *in vitro* models of HD.[28] Undifferentiated SH-SY5Y cells were transduced with LV expressing 18Q (control), 82Q or 82Q in combination with LVs expressing VEGF$_{165}$, Hsp70 or truncated low-affinity nerve growth factor receptor (ΔLNGFR control) at an MOI of 25. Ninety-six hours after transduction, cell death, apoptosis, and Htt aggregate formation were assessed. Cell death was assessed by trypan blue staining (**Figure 2a**). SH-SY5Y cells transduced with 82Q vector alone or in combination with ΔLNGFR vector showed similar levels of cell death (18.31 ± 2.20% and 19.41 ± 2.58% respectively), whereas cells transduced with 82Q + VEGF$_{165}$ showed a significant reduction in cell death to 12.85%, an overall reduction of 29.81%, (*$P < 0.05$, Student's paired *t*-test, $n = 4$) demonstrating a clear neuroprotective effect of VEGF$_{165}$ in this HD model. A similar pattern was observed when investigating apoptosis. Adherent cells were incubated with Hoechst-33342 dye and assessed by fluorescent microscopy for cells demonstrating typical apoptotic morphology. Bright cells displaying condensation/fragmentation of the nuclear material (pyknosis) and formation of apoptotic bodies were classed as apoptotic (**Figure 2b**, top panels). The percentage of apoptotic cells was quantified from 10 fields of view (40× magnification) for each condition. SH-SY5Y cells transduced with 82Q or 82Q + ΔLNGFR LVs showed similar levels of 7.33 and 8.01% apoptotic cells respectively, whereas cells transduced with 82Q + VEGF$_{165}$ LVs showed a significant reduction in apoptotic cells to 4.65%, an overall reduction of 36.6% (***$P < 0.001$, Student's paired *t*-test, $n = 4$).

Transduced SH-SY5Y cells were assessed for Htt aggregates with EM48 antibody and DAB staining. Dark cellular staining indicated the formation of Htt aggregates (**Figure 2c**, top panels). SH-SY5Y cells transduced with 82Q or 82Q + ΔLNGFR LVs demonstrated a similar number of Htt aggregates (15.14 versus 15 average aggregates

Figure 1 Generation of bidirectional lentiviral constructs. (**a**) The HIV-1–based transfer vectors used in this study used a bidirectional promoter system based on the minimal cytomegalovirus promoter (minCMV) and the human phosphoglycerate kinase (hPGK) promoter, thus allowing co-ordinate expression of both reporter and test transgenes from the same vector. These were as originally reported by Amendola *et al.* (2005)[27] but differ in that there is no constitutive transport element (CTE) of the Mason-Pfizer virus included in the upstream cassette that is in antisense orientation to the vector LTR. This modification results in better *in vivo* expression (Mario Amendola, personal communication to V.T.). (**b**) We generated transfer vectors in which the human phosphoglycerate kinase (hPGK) promoter drives expression of either wild-type exon I huntingtin (Htt171-18Q) or mutant huntingtin (Htt171-82Q) fragments, human codon-optimized vascular endothelial growth factor 165 (VEGF$_{165}$), human codon-optimized heat shock protein 70 (Hsp70) or C-truncated low-affinity nerve growth factor receptor (ΔLNGFR). Both huntingtin fragments are 5′ myc tagged. The minCMV promoter drives the expression of the marker transgenes enhanced green fluorescent protein (Htt vectors and negative control 1) or red fluorescent protein (VEGF$_{165}$, Hsp70 vectors and negative control vectors 2 & 3). (**c**) Western blot analysis of 293T cell extracts transfected with either bidirectional 18Q and 82Q vectors (pCMV-eGFP.hPGK-Htt171-18Q and pCMV-eGFP.hPGK-Htt171-82Q) or positive control expression vectors (SIN-PGK-Htt171-18Q and SIN-PGK-Htt171-82Q, gift from Nicole Deglon) confirmed appropriate expression of 18 and 82Q huntingtin protein. Arrows indicate ~33 (195aa) and 50 kD (256aa) proteins respectively detected with anti huntingtin EM48 antibody. (**d**) Expression of Hsp70 was confirmed in 293T cell extracts transfected with pCMV-RFP.hPGK-Hsp70 and Hsp70 positive control (pCMVHsp70, a human non-codon optimized cDNA, gift from Professor RI Morimoto) producing a 70 kD expected protein as detected by anti-Hsp70 antibody. (**e**) Expression of VEGF$_{165}$ was confirmed in 293T cell extracts transfected with pCMV-RFP.hPGK-VEGF$_{165}$. Arrow indicates a 25 kD expected protein detected by anti-VEGF antibody just above a non-specific band also present in non-transfected and negative control samples (pCMV-RFP.hPGK-ΔLNGFR). Expression of DsRed was confirmed with DsRed antibody. Blots for GAPDH were included as loading controls. (**f**) An ELISA confirmed the presence of VEGF in the supernatant of 293T cells transduced with pCMV-RFP.hPGK-VEGF$_{165}$. (**g**) Coexpression of 82Q and VEGF$_{165}$ in 293T cells cotransduced with pCMV-eGFP.hPGK-Htt171-82Q and pCMV-RFP.hPGK-VEGF$_{165}$ at an MOI of 10.

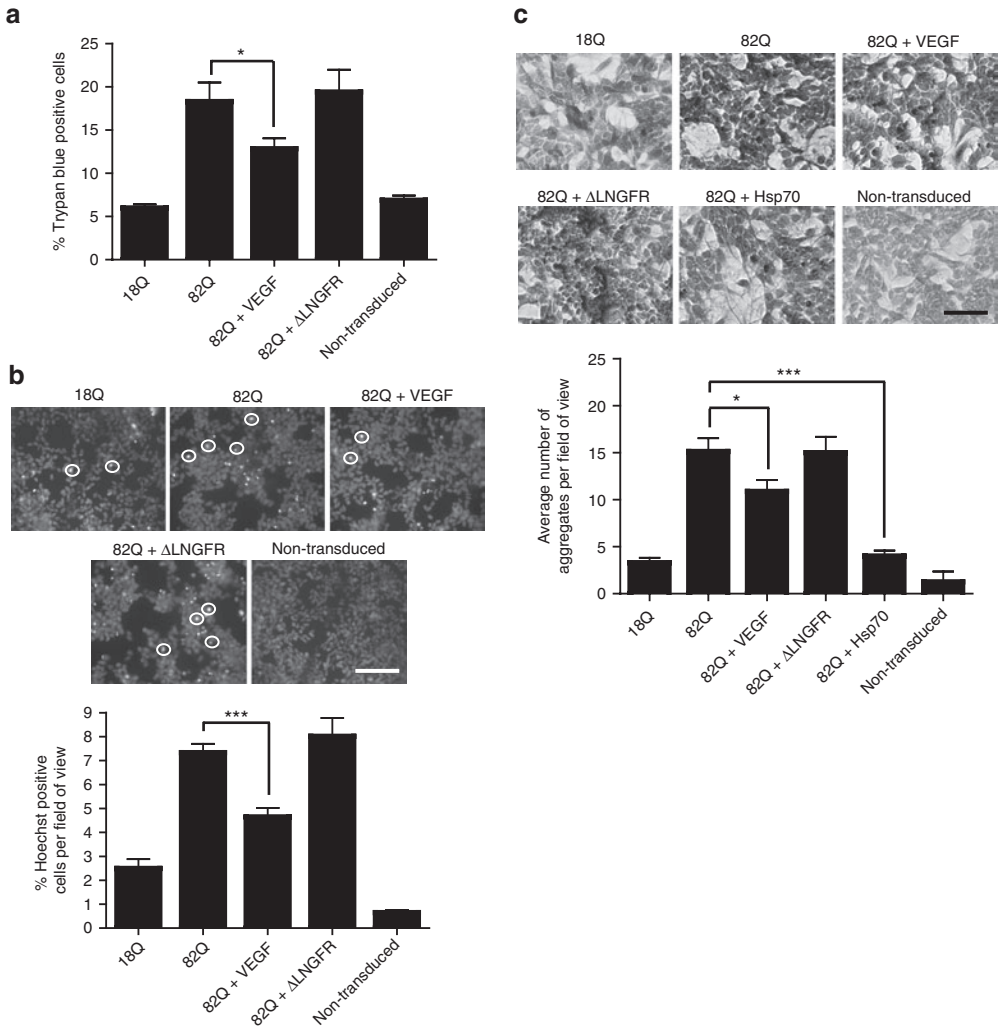

Figure 2 Neuroprotective and anti-aggregating effects of vascular endothelial growth factor 165 (VEGF$_{165}$) in an *in vitro* SH-SY5Y model of Huntington's disease. (**a**) SH-SY5Y neuroblastoma cells were transduced with lentiviral vector expressing wild-type Htt (18Q), Exp-Htt (82Q) alone or in combination with lentiviral vector encoding human VEGF$_{165}$ (82Q + VEGF) or control lentiviral vector (82Q + ΔLNGFR). Ninety-six hours after transduction, cell death was assessed by trypan blue staining. Expression of VEGF with 82Q showed a significant reduction in trypan blue positive cells compared with 82Q alone ($n = 4$, mean ± SEM, $^*P < 0.05$, Student's *t*-test). Equivalent levels of trypan blue positive cells were observed in the non-transduced and 18Q-transduced groups. (**b**) The experiment was repeated and cell apoptosis assessed by Hoechst dye staining. Bright staining indicated cells undergoing apoptosis (examples of apoptotic cells circled). Coexpression of VEGF with 82Q showed a significant reduction in Hoechst positive cells compared with 82Q alone ($n = 4$, mean ± SEM, $^{***}P < 0.001$, Student's *t*-test). (**c**) SH-SY5Y cells were transduced with lentiviral vector encoding wild-type Htt (18Q), Exp-Htt (82Q) alone or in combination with lentiviral vector encoding human VEGF$_{165}$ (82Q + VEGF), negative control lentiviral vector (82Q + ΔLNGFR) or positive control lentiviral vector encoding Hsp70 (82Q + Hsp70). Ninety-six hours after transduction, the formation of huntingtin inclusions was assessed by EM48 antibody and DAB staining. Quantitative analysis demonstrates that coexpression of VEGF with 82Q significantly reduced the number of huntingtin aggregates compared with 82Q alone ($n = 4$, mean ± SEM, $^*P < 0.05$, Student's *t*-test). Scale bars represent 50 µm.

per field of view, 40× magnification), whereas cotransduction with 82Q + VEGF$_{165}$ LV resulted in a reduction in aggregate number to 10.89 (an overall reduction of 28.1%), demonstrating VEGF$_{165}$ is anti-aggregating in this model. A positive anti-aggregating effect of Hsp70 was also observed in this HD model.[6,8] Cotransduction of Hsp70 and 82Q vectors resulted in a reduction in aggregate formation by 73.6% as compared with the 82Q only transduced cells.

VEGF$_{165}$ is neuroprotective in an 82Q striatal neuronal culture model while Hsp70 is anti-aggregating

We further investigated the potential of our bidirectional lentiviral system to generate a long-term *in vitro* model of HD using rat primary striatal cultures.[23] Striatal neurons grown in primary culture (NeuN$^+$/DARPP32$^+$ data not shown), demonstrate a range of neurochemical phenotypes and cell–cell interactions which correspond closely to those present in the mature striatum *in vivo*.[29] Primary striatal neuronal cultures were transduced with 82Q LV alone or in combination with VEGF$_{165}$, Hsp70, or ΔLNGFR LVs. Controls were transduced with 18Q or ΔLNGFR LVs coexpressing eGFP or RFP reporters. Six weeks after transduction cells were stained with the neuronal marker NeuN to assess cell survival and the Htt aggregate marker EM48 (**Figure 3**). Neurons transduced with 82Q LV showed a significant reduction in number compared with those transduced with 18Q and ΔLNGFR LVs (5.71 versus

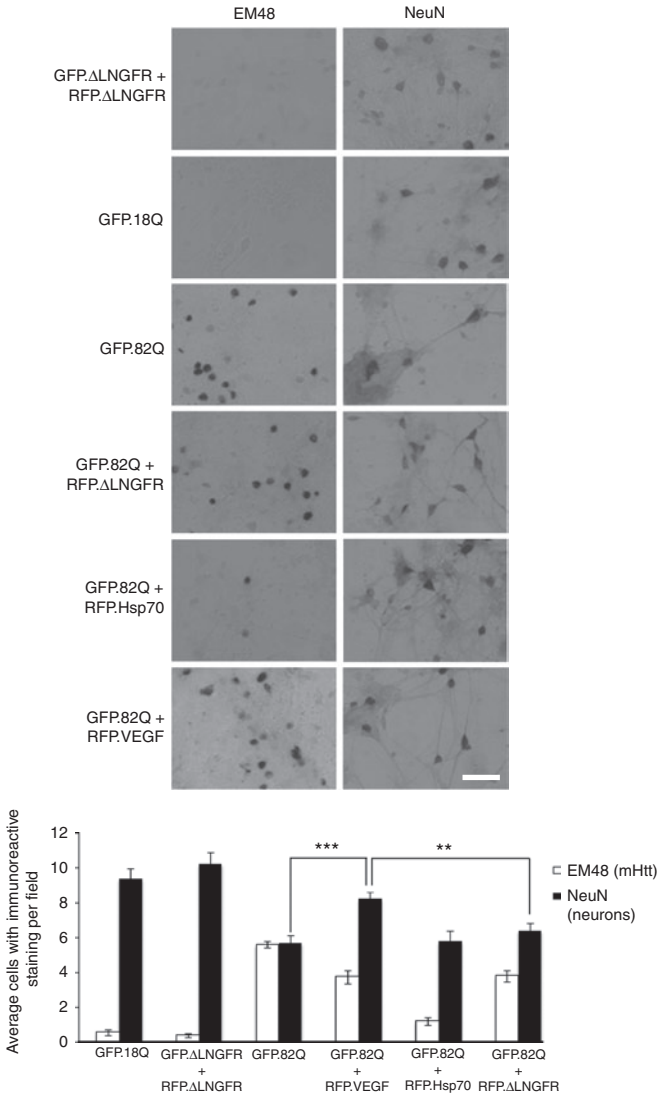

Figure 3 Neuroprotective effects of vascular endothelial growth factor 165 (VEGF$_{165}$) in an *in vitro* primary striatal neuronal culture model of Huntington's disease. Primary striatal neuronal cultures were transduced with lentiviral vectors encoding ΔLNGFR or 18Q as controls and 82Q alone or in combination with ΔLNGFR, Hsp70 or VEGF$_{165}$. Six weeks after transduction striatal cultures were fixed and stained for huntingtin aggregates (EM48 antibody) and NeuN followed by DAB staining. Huntingtin aggregates were observed in all groups expressing 82Q, but a reduction of aggregates was observed in cells cotransduced with 82Q and the positive control Hsp70. Neuronal survival was assessed with NeuN staining. Striatal neuronal cultures coinfected with 82Q and VEGF showed a significant enhancement of cell survival compared with 82Q alone ($n = 3$, mean ± SEM, ***$P < 0.001$, Student's t-test) and 82Q plus Hsp70 or ΔLNGFR control ($n = 3$, mean ± SEM, **$P < 0.01$, one way analysis of variance). Scale bar represents 50 µm.

9.36 and 10.21 mean NeuN$^+$ cells respectively). This cell death was partly restored when cells were coinfected with 82Q and VEGF$_{165}$. Cotransduction with VEGF$_{165}$ LV resulted in a significant increase of 28.8% in the number of surviving neurons compared with controls, demonstrating substantive neuroprotection from 82Q toxicity in this progressive *in vitro* HD model. In accordance with previous reports, Hsp70 was not found to be neuroprotective in cells cotransduced with 82Q and Hsp70;[8] however, Hsp70 did significantly reduce the number of 82Q aggregates as detected with EM48 staining (5.61 average aggregates for 82Q alone versus 1.23 average aggregates for 82Q + Hsp70, a reduction of 78.2%). In the 82Q + VEGF$_{165}$–transduced neurons a reduction in aggregates was observed compared with 82Q alone (3.77 versus 5.61 respectively); however, this reduction was not significant when compared with the 82Q + ΔLNGFR control group (82Q + VEGF$_{165}$: 3.77 versus, 82Q + ΔLNGFR: 3.84 average aggregates).

LV PolyQ expression induces aggregation and neurotoxicity in the striatum *in vivo*

We next attempted to generate a lentiviral-mediated *in vivo* model of HD using our novel bidirectional LVs.[25] Rats were stereotaxically injected in the right striatum with 82Q vector to induce biochemical features of HD. Preliminary studies demonstrated striatal Htt aggregate formation without neurotoxicity at 5 weeks and increased aggregate formation with striatal neurodegeneration at 8 weeks after transduction (1.25 µl of 82Q LV, 6.78×10^8 TU/ml, 1.11×10^5 ng p24/ml) (**Supplementary Figure S1**). On the basis of these initial observations, we increased the 82Q LV dose (4 µl, 1.33×10^9 TU/ml, 7.87×10^3 ng p24/ml) and tested incubation times of 8, 10, or 12 weeks to achieve optimal neurotoxicity and Htt aggregate formation in the striatum (**Figure 4**). Targeted transduction of 82Q LV within the striatum was confirmed by immunohistochemistry with GFP antibody staining (**Figure 4a**). In this experiment, the 10-week time point demonstrated maximal DARPP-32 depletion (**Figure 4a–e**), with almost twofold increase in damaged area compared with the 8-week time point (10 week: 3.34 mm^3 versus 8 week: 1.89 mm^3). Extending the incubation period to 12 weeks did not increase the area of DARPP-32 depletion. The maximal number of Htt aggregates was also detected at the 10-week time point as detected with 2B4 antibody and did not increase with increasing incubation time (average number of aggregates for 82Q-transduced brains = 3,214 ± 1,289 $n = 3$ **Figure 4f–i**). For Htt aggregates detection *in vivo*, the 2B4 antibody provided less background than EM48 antibody staining. The huntingtin inclusions detected costained for ubiquitin and c-Myc antitag antibody (**Figure 4j–m**) and appeared to be predominantly nuclear following confocal microscopy analysis corresponding to previous reports (**Figure 4n–q**).[25] No DARPP-32 depletion or Htt aggregates were detected in control brains transduced with 18Q LV as expected (**Figure 4b**,**f**). These findings confirmed sufficient neurotoxicity and Htt aggregate formation at 10 weeks after transduction in this *in vivo* HD model.

Coexpression of 82Q and low dose VEGF$_{165}$ attenuates neurodegeneration in the rat striatum

To determine whether VEGF$_{165}$ confers neuroprotection in our *in vivo* HD model, rats were coinjected with 82Q and VEGF$_{165}$ LVs into the right striatum and compared with an 82Q plus control ΔLNGFR coinjected group. Ten weeks after transduction, a marked decrease in neurodegeneration within the striatum, as determined by DARPP-32 immunohistochemistry, was observed in the 82Q + VEGF$_{165}$–coinjected group (**Figure 5a**). The total volume of DARPP-32 depletion was significantly smaller in the presence of VEGF (82Q + ΔLNGFR: 4.385 ± 0.56 mm^3 versus 82Q + VEGF 2.79 ± 0.18 mm^3; *$P < 0.05$, $n = 4$). VEGF expression

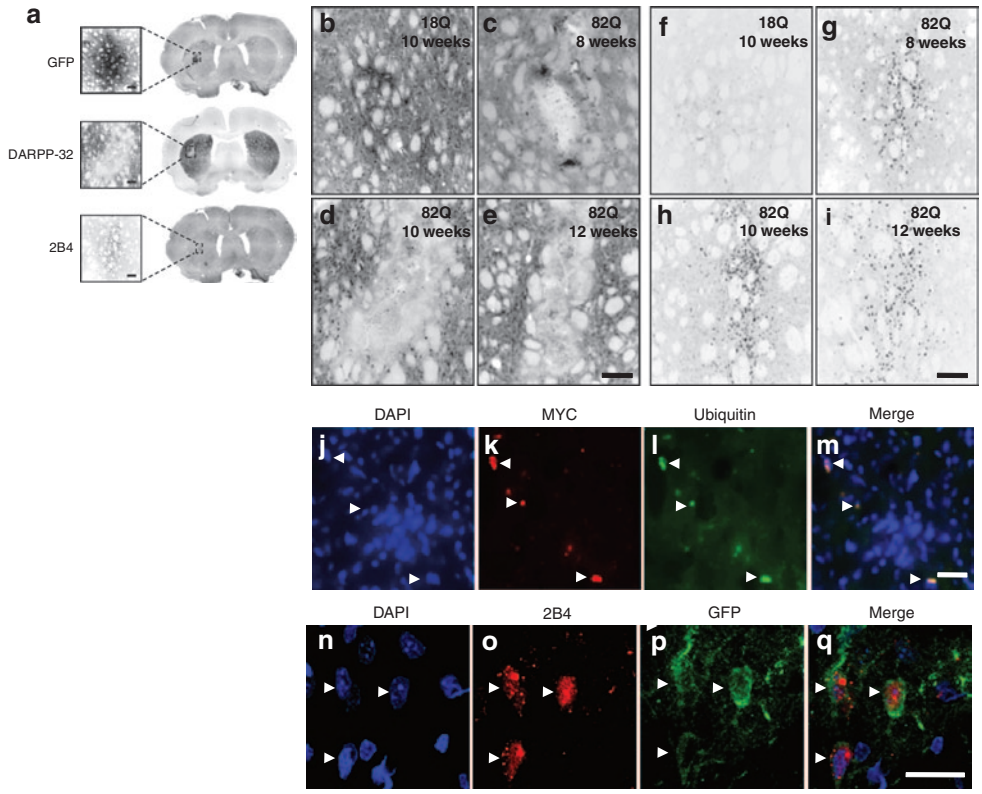

Figure 4 Generation of an *in vivo* model of 82Q striatal aggregation and toxicity. Wistar rats were transduced in the striatum with 18Q or 82Q expressing LV by sterotaxic injection and examined 8, 10, or 12 weeks after transduction (n = 6). (**a**) Representative coronal sections of the striatum demonstrating GFP expression, DARPP-32 depletion and 2B4 stained huntingtin aggregates from a GFP.82Q LV–injected rat (4× tiled images). (**b**–**e**) Evaluation of the neurotoxicity of 18Q (10 weeks) and 82Q (8, 10, and 12 weeks) on DARPP-32 stained striatal sections. As expected, no striatal degeneration was observed in the 18Q-transduced striatum. Most significant striatal degeneration was observed at the 10-week time point in the 82Q-transduced striatum. (**f**–**i**) No Htt inclusions were detected in the 18Q-transduced striatum with 2B4 antibody. The highest level of huntingtin inclusions were detected in the 82Q-transduced striatum at the 10-week time point. Scale bars represent 100 µm (**j**–**m**) DAPI, c-Myc (MYC) and ubiquitin triple staining indicates that huntingtin inclusions (c-Myc tagged) are ubiquitinated. Scale bar represents 25 µm. (**n**–**q**) DAPI, 2B4 and GFP triple staining indicates the presence of nuclear Htt inclusions within 82Q-transduced neurons. Scale bar represents 25 µm.

reduced the volume of polyQ-induced DARPP-32 depletion by 36.4%. There was a similar reduction in striatal degeneration observed with NeuN staining (Figure 5a), a late marker of neuronal dysfunction in LV-based HD rat models.[30] The total volume of NeuN depletion for 82Q + ΔLNGFR was 2.554 ± 0.22 mm^3 compared with 82Q + VEGF area of 1.564 ± 0.08 mm^3, an improvement of 38.8%. We then analyzed the number of Htt aggregates present within the striatum of both groups and observed an overall decrease in 2B4 stained aggregates in the 82Q + VEGF$_{165}$ group compared with 82Q + ΔLNGFR control group (Figure 5b) (mean aggregates 3,668 ± 595.1 versus 6,701 ± 570.3, a 45.3% reduction in the presence of VEGF$_{165}$).

VEGF$_{165}$ has been previously reported to activate astrocytes.[31,32] We therefore looked for activated astrocytes using the glial specific marker glial fibrillary acidic protein (GFAP). Activated astrocytes were observed in both groups in and around the site of injection/needle tract (cortex, corpus collosum, and striatum on ipsilateral side) and also along the corpus collosum on the contralateral side to similar extents (Figure 5c). A small increase in activated astrocytes was observed in the 82Q + VEGF$_{165}$ group near the epicentre of injection which could be attributed to activation by VEGF$_{165}$ (Figure 5c, left panels); however, extensive astrogliosis was not observed in the 82Q + VEGF$_{165}$ group. A similar anteroposterior spread of vector throughout the striatum, as characterized by eGFP expression, was observed between both groups indicating the differences in neurodegeneration and aggregate formation detected were not attributed to a difference in 82Q LV injected (Figure 5d) (anterior/posterior LV spread: 82Q + ΔLNGFR 2,280 µm versus 2,400 µm 82Q + VEGF).

Interestingly, rats receiving 82Q + VEGF gained more weight during the 10-week incubation compared with the 82Q + ΔLNGFR control group (Figure 5e), further emphasizing the positive effect of VEGF$_{165}$ in HD pathology. No adverse inflammatory response (as assessed by ED1 and CD4 markers), vascularization (Glut-1 marker) or vascular leakage (albumin staining) were detected (Figure 7b and data not shown). These findings suggest LV delivery of VEGF$_{165}$ may have potential therapeutic application in the treatment of HD.

Coexpression of 82Q and high dose VEGF$_{165}$ in the rat striatum causes overt toxicity and chronic inflammation

To see if the extent of VEGF$_{165}$-induced neuroprotection could be improved upon, we coinjected 82Q with a higher dose of VEGF$_{165}$

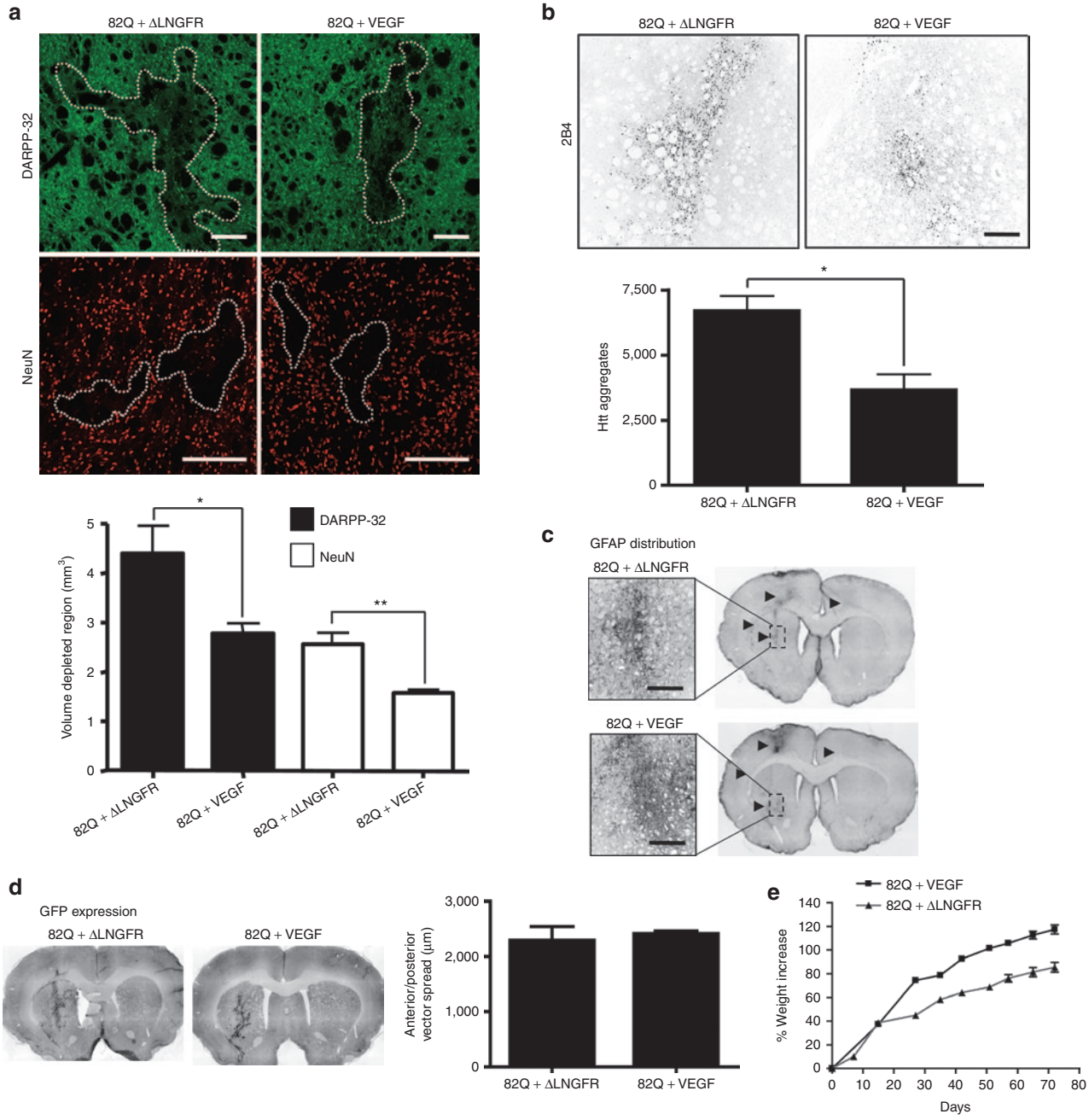

Figure 5 Neuroprotective and anti-aggregating effects of low dose vascular endothelial growth factor 165 (VEGF$_{165}$) in an *in vivo* model of HD. (**a**) Immunocytochemical detection of DARPP-32 (top panels) and NeuN (bottom panels) was performed with specific antibodies (see Materials and Methods). 82Q-induced neurodegeneration confirmed by DARPP-32 and NeuN depletion is attenuated by VEGF expression. Graphical representation of the total volume depletion for DARPP-32 and NeuN for 82Q + ΔLNGFR control and 82Q + VEGF–infected striatums ($n = 4$, mean ± SEM, $^*P < 0.05$, $^{**}P < 0.001$, Student's paired *t*-test). (**b**) The number of striatal 82Q-induced Htt aggregates was significantly reduced by coexpression of VEGF ($n = 4$, mean ± SEM, $^*P < 0.05$, Student's paired *t*-test, 82Q + ΔLNGFR control versus 82Q + VEGF infection). (**c**) Reactive astrocytes were assessed by GFAP staining (82Q + ΔLNGFR control versus 82Q + VEGF infection). Reactive astrocytes were observed in both groups around the sites of injection in the cortex, corpus collosum and the striatum (arrow heads). (**d**) Striatal 82Q vector spread as determined by GFP reporter expression is equivalent for both 82Q + ΔLNGFR control and 82Q + VEGF–transduced groups ($n = 4$, mean ± SEM). (**e**) Percentage weight increase of animals following 82Q + VEGF or 82Q + ΔLNGFR injection. Scale bars represent 200 μm.

LV (tenfold higher titer) to increase the overall amount of VEGF$_{165}$ expression. A striking observation from these brains harvested 10 weeks after injection was that rats receiving the 82Q coinjection with the higher dose of VEGF$_{165}$ suffered from an enlarged/swollen brain (~25% increase in size), along with a hemorrhagic legion around the injection site which was not observed in the control group (Figure 6a) nor the 82Q + lower dose VEGF$_{165}$ group. Coinjection with high dose VEGF$_{165}$ also caused a reduction in overall body weight increase compared with 18Q, 82Q, and 82Q + ΔLNGFR control groups (Figure 6b). VEGF$_{165}$ is well described

for its role in angiogenesis and vascular permeabilization.[17,33] We therefore assessed whether an overexpression of VEGF$_{165}$ in this system causes adverse vascularization and blood leakage. Endothelial glucose transporter-1 (Glut-1), a specific blood–brain barrier (BBB) marker protein was used to determine vascularization. Secreted VEGF$_{165}$ is known to increase glucose transport across the BBB.[34,35] Glut-1 positive microvessels were detected within the striatum around the injection site and in more distant areas of the striatum (**Figure 6c**) indicating vascularization and BBB disruption. The entire brain was then assessed for blood albumin protein leakage (**Figure 6d**). A striking observation following sectioning was a large intracranial cavity containing necrotic tissue originating from the site of injection. Extensive damage throughout the brain was observed affecting predominantly the

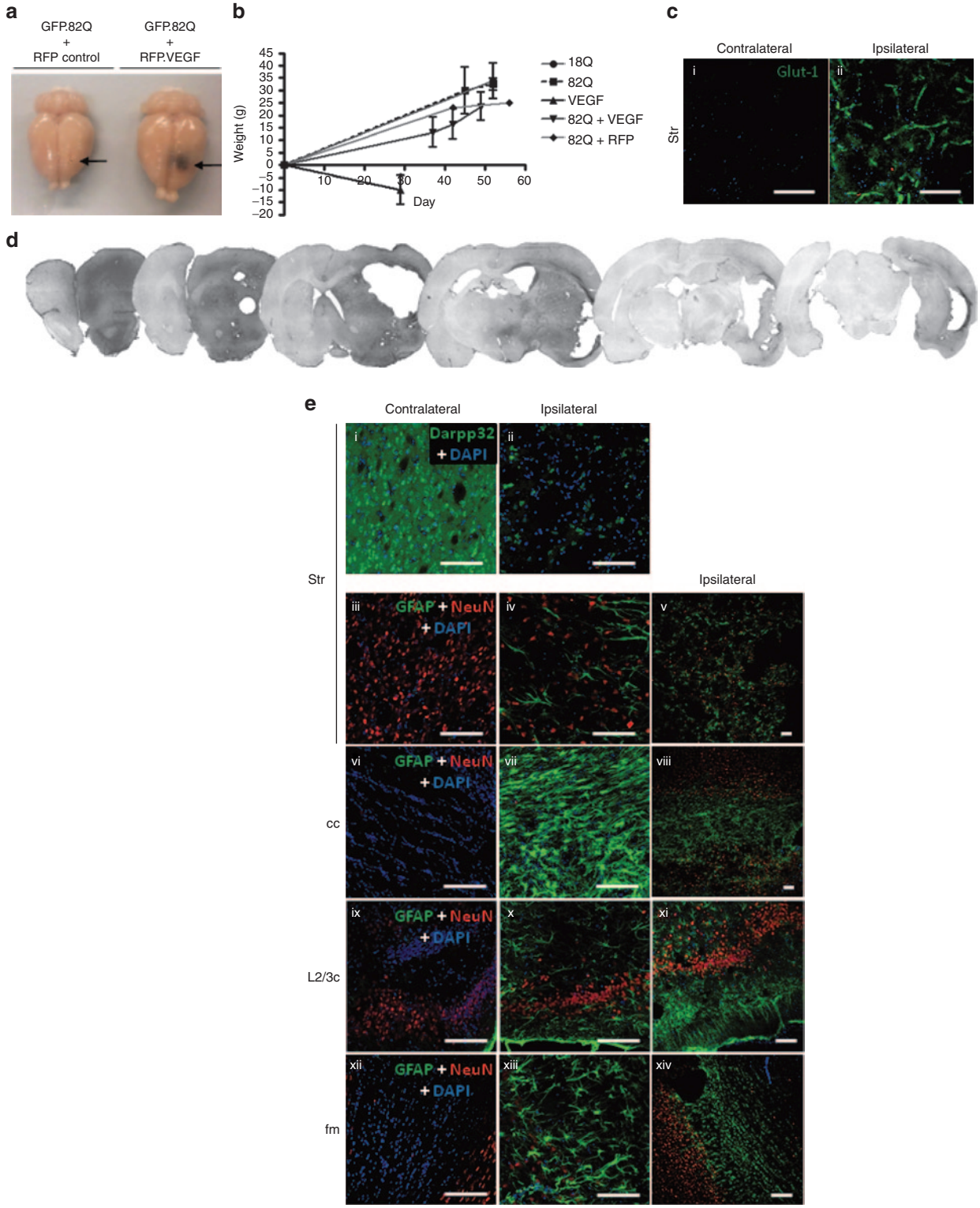

striatum, corpus collosum, and interconnecting forceps major (**Figure 6d**). This was accompanied with an extensive amount of blood albumin leakage which appeared to be largely restricted to the ipsilateral side but extended throughout the brain from early anterior to posterior brain regions (**Figure 6d** dark staining). There was also an enlargement of the brain on the ipsilateral side. These findings indicate that lentiviral-mediated VEGF$_{165}$ overexpression has serious consequences for BBB permeability and tissue necrosis in the rat brain which override the neuroprotective effects observed at a lower dose.

We next assessed neurodegeneration and astrogliosis (**Figure 6e**). A large proportion of the striatum suffered extensive necrosis and the remaining striatum showed a dramatic reduction in DARPP-32 positive medium spiny neurons compared with the contralateral side (**Figure 6e**; i,ii). This was accompanied with a large reduction of NeuN$^+$ cells in the ipsilateral striatum (**Figure 6e**; iv). NeuN staining in the striatum on the contralateral side appeared normal suggesting there was little or no neurodegeneration on the contralateral side (**Figure 6e**; iii). In the CNS, glial cells greatly out-number neurons, not only playing a supporting role in essential neuronal function but also acting as primary responders to CNS insults such as infection, injury and degenerative disease.[36] We observed a widespread infiltration of GFAP$^+$ reactive astrocytes in the damaged striatum (**Figure 6e**; iv,v), corpus collosum (**Figure 6e**; vii,viii) and ventral regions of the brain including layer 2/3 cortex (**Figure 6e**; x,xi). The most concentrated region of reactive astrocytes was observed in the corpus collosum adjacent to the most severe area of damage affecting the corpus collosum and striatum (**Figure 6e**; vii). The corpus collosum connects the two hemispheres of the brain and also extends to the brain posterior connecting to the forceps major. No reactive astrocytes were observed on the contralateral side corpus collosum (**Figure 6e**; vi); however, they were detected extensively in the forceps major on the ipsilateral side (**Figure 6e**; xiii,xiv). The extensive amount of astrogliosis observed is most likely due to a combination of VEGF$_{165}$-induced activation and proliferation of astroglia in response to the large amount of neurodegeneration observed.

We then investigated whether there had been any inflammatory response to VEGF$_{165}$ overexpression by examining various inflammatory markers such as macrophages/monocytes (ED1), T helper cells, monocytes, macrophages and dendritic cells (CD4 glycoprotein) and cytotoxic T cells (CD8). We found significant macrophage/monocyte infiltration in the ipsilateral striatum, corpus collosum, forceps major and piriform cortex brain regions (**Figure 7a**; ii,vi,x,xiv), whereas none were observed on the contralateral side (**Figure 7a**; i,v,ix,xiii). VEGF$_{165}$ is a chemoattractant to monocytes and can induce their migration across collagen membranes and endothelial cell monolayers.[37] A similar pattern of infiltration was observed following staining with antibody against CD4 glycoprotein, with large amounts of CD4$^+$ cells detected in ipsilateral striatum, corpus collosum, forceps major and to a lesser extent piriform cortex (**Figure 7a**; iii,vii,xi,xv). A small number of cytotoxic T cells (CD8$^+$) were detected within the striatum near the area of damage but not in other regions (**Figure 7a**; iv,viii,xii,xvi). These findings are in direct contrast to low dose VEGF$_{165}$ where no ED1 or CD4$^+$ cells were detected (**Figure 7b**).

To ensure that the dramatic inflammatory responses observed here were not caused by LV contamination 18Q, 82Q, and VEGF$_{165}$ LV preps were tested for endotoxin, bacterial and mycoplasma contamination (see Materials and Methods). No contamination or abnormal endotoxin levels were detected in any of the LV preps. These results indicate the vascular properties of unregulated vector–mediated VEGF$_{165}$ expression override its neuroprotective ones at a certain dose leading to inflammation and neurotoxicity instead and thus raises important safety implications for unregulated CNS applications with this factor.

VEGF$_{165}$ overexpression in the striatum leads to neurotoxicity and death

As a control, three rats were injected with the same high dose of VEGF$_{165}$ LV unilaterally in the striatum. In the absence of Exp-Htt, VEGF$_{165}$ overexpression proved to have more severe adverse side effects including progressive weight loss, akinesia and cyphosis in all injected animals. This led to premature death in two of the animals after just 3 weeks. The third animal was euthanatized and processed shortly after. *Post mortem* examination revealed similar but far more global brain pathology to that observed in the VEGF$_{165}$ + 82Q coinjected brains with neurodegeneration, vascular leakage, and astrogliosis spreading further anteroposterior from the injection site ipsilaterally and being more prominent on the contralateral side (**Supplementary Figure S2a,b**). Neuroinflammation was also more prominent with a greater influx of macrophages/monocytes observed on the contralateral side (**Supplementary Figure S3**). We speculate that coexpression of mHtt reduces expression of VEGF$_{165}$ from the transduced striatum thus reducing its deleterious side effects.

DISCUSSION

For this study, we used a novel bidirectional HIV-1 LV approach to study the therapeutic potential of the human isoform of VEGF-A, VEGF$_{165}$, to protect against neurodegeneration in both *in vitro* and *in vivo* models of HD. We successfully constructed

Figure 6 Acute striatal toxicity and vascularization with high dose vascular endothelial growth factor 165 (VEGF$_{165}$) in an *in vivo* model of HD. (**a**) Transduction with 82Q + high dose VEGF LV caused extensive brain swelling and hemorrhage. Arrows indicate site of injection and necrotic lesion. There was no adverse phenotype observed in the 82Q + RFP control–infected group (n = 6). (**b**) 82Q + high dose VEGF–injected rats gained less weight compared with 18Q, 82Q and 82Q + RFP control–infected groups. Rats receiving high dose VEGF LV alone lost body weight and perished before 4 weeks due to adverse affects (see **Supplementary Figures S2 and S3**). (**c**) Glut-1 staining demonstrated extensive vascularization in the striatum of the 82Q + high dose VEGF–injected brain on the ipsilateral side. (**d**) Vascular leakage was assessed by sectioning the entire brain and staining for albumin (dark staining). Extensive vascular leakage was present, predominantly on the ipsilateral side. Significant tissue damage was observed in the striatum and corpus collosum originating from the site of injection. (**e**) Neurodegeneration and astrogliosis were assessed by DARPP-32, NeuN, and GFAP staining, with DAPI counter staining. (i,ii) Extensive DARPP-32 loss (green staining) was observed in the ipsilateral striatum (str), whereas strong DARPP-32 staining was observed in the contralateral striatum. (i,iii) A large number of vacuoles were observed on the contralateral side. (iv,v) Extensive NeuN loss was observed in the ipsilateral striatum, along with extensive astrogliosis. Activated astrocytes (GFAP, green staining) were observed in the (vii,viii) ipsilateral corpus collosum (cc), (x,xi) layer2/3 cortex (L2/3c), and (xiii,xiv) forceps major (fm). (iii,vi,ix,xii) Astrogliosis was not observed on the contralateral side. Scale bar represents 100 μm.

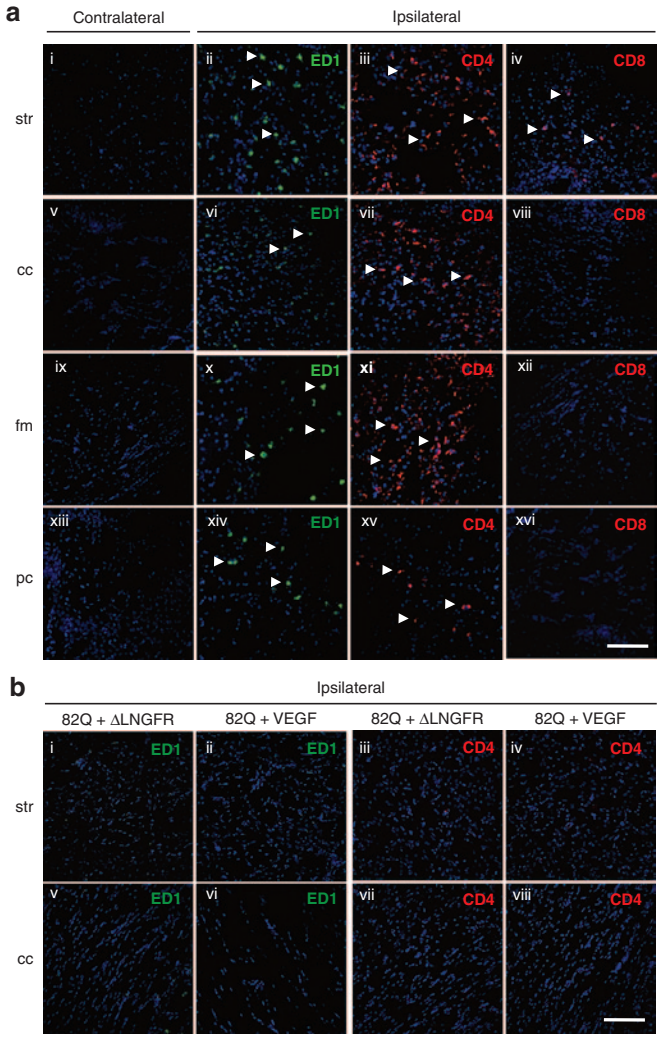

Figure 7 Extensive neuroinflammation with high dose vascular endothelial growth factor 165 (VEGF$_{165}$) in an *in vivo* model of HD. (**a**) 82Q + high dose VEGF–injected brains: widespread macrophages/monocyte (ED1, green staining) and CD4$^+$ T cell (CD4, red staining) infiltration was observed in the ipsilateral side in regions such as the (ii, iii) striatum (str), (vi, vii) corpus collosum (cc), (x, xi) forceps major (fm), and (xiv,xv) piriform cortex (pc). (iv) Some cytotoxic T cells were also observed in the striatum close to the site of injection. No inflammatory markers were detected on the contralateral side (i,v,ix,xiii). (**b**) 82Q + low dose VEGF–injected brains: No macrophage/monocyte infiltration (ED1, green staining) or CD4$^+$ T cells (CD4, red staining) were observed in the striatum (str) or corpus collosum (cc) of rats injected with either 82Q + ΔLNGFR or 82Q + low dose VEGF (i–viii). Scale bar represents 100 µm.

efficient bidirectional LVs enabling us to set up *in vitro* and *in vivo* HD models and test new gene therapies in them. Their application produced similar effects to those seen with alternate vector systems.[23,25]

Using LV-mediated overexpression of mHtt, we were able to generate two *in vitro* models of HD; a fast, aggressive HD model by infecting neuronal-like SH-SY5Y cells with a high MOI (25) of 82Q LV and a slower, more progressive primary striatal neuron HD model by transducing with 82Q LV at a lower MOI (10). In both models, we demonstrated a clear neuroprotective role of VEGF$_{165}$ against Exp-Htt–induced cytotoxicity. In the SH-SY5Y HD model, LV-mediated overexpression of VEGF$_{165}$ reduced cell death and apoptosis by a third, likewise VEGF overexpression in primary striatal neurons expressing htt171-82Q improved neuronal survival by a similar degree. These encouraging observations are in accordance with previous *in vitro* studies which highlight VEGF$_{165}$ as a neuroprotective growth factor in cortical, hippocampal, motor, retinal, and dopaminergic neurons following polyglutamine-induced toxicity or hypoxia.[33,38–44]

In a generated *in vivo* HD model, we were able to replicate the neuroprotective role of VEGF$_{165}$ observed in the *in vitro* experiments, by cotransduction with a low dose of LV. Promisingly, striatal neurodegeneration, induced by LV-mediated mHtt overexpression, was attenuated by VEGF expression, as assessed by early and late markers of striatal degeneration, DARPP-32 and NeuN. These results highlight the therapeutic potential of lentiviral-mediated delivery of VEGF in HD to reduce Exp-Htt–induced neurodegeneration. The capacity of VEGF$_{165}$ as a therapeutic for other neurodegenerative diseases such as ALS has been previously explored with positive outcome. VEGF delayed neurodegeneration and prolonged survival in ALS mice,[19] consistent with findings observed in SOD1^{G93A}/VEGF$^{+/+}$ double transgenic mice.[45] Intrastriatal delivery of VEGF by AAV vector has shown to be beneficial in models of Parkinson's disease, promoting survival of dopaminergic neurons and improving rotational behavior.[46] Notably, a significant astrocytic infiltration was observed in this study. In a more recent study, the delivery of VEGF$_{165}$ via injectable hydrogels, to rats receiving striatal injection of quinolinic acid to mimic neuronal loss and behavioral deficits characteristic of HD, was shown to be neuroprotective at 3 weeks.[47] The advantage of our HD model over others is the expression of mHtt in the striatum which replicates the human pathology of the disease more closely, resulting in both progressive striatal neurodegeneration and aggregate formation. Also, using LVs as a therapeutic delivery system for VEGF$_{165}$, or indeed other therapeutic genes, has the distinct advantage of providing long-term gene expression abolishing the need for repeat treatments. Although not directly comparable due to different delivery systems and disease models, these studies and our own findings demonstrate the favorable effects of VEGF as a therapeutic in neurodegenerative diseases including HD. Furthermore, no adverse side effects of VEGF expression such as vascular leakage, vascularization, or immune response were reported similar to our observations with a low dose of VEGF LV.

In addition to neuroprotection, we also observed an unexpected VEGF-dependent anti-aggregating effect in both the SH-SY5Y and *in vivo* HD models, which to our knowledge is the first observation of its type. The exact mechanism of how VEGF has reduced aggregate formation is unclear from our studies and requires further investigation. Interestingly, in other acute and chronic models of HD, the neurotrophic factors, ciliary neurotrophic factor and brain-derived neurotrophic factor, have also shown to be neuroprotective, ameliorating striatal degeneration,[13,48] but without modifying inclusion formation.

In this study, we tried to maximize the neuroprotective and anti-aggregating effects of VEGF$_{165}$ in our *in vivo* HD model by increasing the dose but dramatically, overexpression of VEGF$_{165}$ caused extensive, adverse side effects including tissue damage,

hypertrophy, vascular leakage, vascularization, astrogliosis, and neuroinflammation which overshadowed the beneficial effects observed at the lower dose. Similar unanticipated pleiotropic effects following high dose administration of VEGF to the adult CNS, have been reported using different delivery systems. Administration of human recombinant $VEGF_{165}$ by osmotic minipump and subdural sponge placement has been shown to cause cerebral angiogenesis, extensive protein leakage, BBB permeability, and proliferation of astroglia.[35] Also chronic overexpression of $VEGF_{165}$ by intracerebral infusion via miniosmotic pump or intracerebral injection of an adenoviral vector encoding $VEGF_{165}$ increased BBB permeability and inflammation in wild-type rat brain.[49] In addition, astrocyte-derived VEGF-A was shown to mediate BBB disruption, lymphocyte infiltration, and tissue damage in CNS inflammatory disease.[50] These observations taken together with our findings demonstrate that $VEGF_{165}$ expression can be both beneficial and detrimental in the brain dependent on the dose and method of administration.

The mechanism by which $VEGF_{165}$ exerts its neuronal survival effects appears to be via signaling through VEGFR2, PI3-kinase/Akt, and MEK/ERK predominantly but also via regulation of potassium channels which are dependent on VEGFR1 signaling.[38] Interestingly, vasopermeability, cell proliferation, and angiogenesis are also triggered via VEGFR2 signaling but through activation of PLCγ. This suggests that a dose-dependent threshold of VEGF may exist which tips the balance from neurosurvival/protection to vasopermeability and neurotoxicity.

MATERIALS AND METHODS

Cells. Cell lines, 293T cells (HEK 293T/17, ATCC CRL-11268), were grown in Dulbecco's modified Eagles medium (Sigma, St Louis, MO; D6546) supplemented with Penicillin/Streptomycin (Pen/Strep; Sigma; P4333), 4 mmol/l L-glutamine (Sigma; G7513), and 10% (v/v) new born calf serum (Sigma; N4762). SH-SY5Y (ECACC, 94030304) cells were maintained in 1:1 Ham's F12 (Sigma; N4888): Eagle's minimal essential medium (Sigma; M2279) supplemented with 2 mmol/l glutamine, 1% non essential amino acids, and 15% fetal bovine serum. Primary striatal cells were prepared as follows: timed-pregnant Sprague–Dawley rats (Charles Rivers Laboratories, Les Oncins, France) were killed by CO_2 inhalation, and embryos (E16) were collected in a Petri dish and placed on ice. Dissections were performed under a stereomicroscope in ice-cold dissection medium (DMX) containing Ca^{2+}- and Mg^{2+}-free phosphate-buffer saline (PBS), 0.6% D-glucose, 1% Pen/Strep (10,000 U/ml, 10,000 Ag/ml), and 10 mmol/l HEPES (Invitrogen, Carlsbad, CA). Ganglionic eminences or cerebral cortices were isolated, cut into pieces using forceps, and collected in a 15 ml Falcon tube. The medium and buffer were removed by decanting on ice. The tissue was homogenized by repeated pipetting with a fire-polished Pasteur pipette in DMX containing 1% bovine serum albumin (Sigma). Cells were centrifuged at 4 °C for 5 minutes at 1,000*g* and resuspended in 10 ml of glutamate-free Neurobasal medium containing 1% B27 (Invitrogen), 2% Pen/Strep (10,000 U/ml, 10,000 Ag/ml), 0.5 mmol/l L-glutamine, and 15 mmol/l KCl. Cells were plated at a density of 150,000 cells/cm^2 in multi-well dishes coated with 20 µg/ml poly-L-lysine (Sigma; P6407). The cultures were maintained in a humid incubator (5% CO_2 at 37 °C), and half of the medium was changed weekly. Cultures were kept for up to 6 weeks.

Cloning and generation of transfer vector plasmids. Transfer vector plasmids encoding the genes of interest (htt171-18Q, htt171-82Q, and $VEGF_{165}$) and reporter genes (either GFP or RFP) (**Figure 1**) were generated by cloning into the bidirectional promoter vector, pCCL.sin_PPT.SV40polyA.GFP.minhCMV.hPGK-ΔLNGFR.WPRE, which was kindly provided by Mario Amendola (San Raffaele Telethon Institute for Gene Therapy, HSR-TIGET, Milan, Italy). p889-HD-N171-Myc (18Q) and p926-HD-N171-Myc (82Q) plasmids encoding wild-type and mutant fragment of the N terminal (171aa) htt gene respectively were kindly provided by Nicole Deglon (Commissariat á l'Energie Atomique, Orsay Cedex, France). htt171-18Q and 82Q were subcloned into pBluesript II KS (+) to add additional restriction sites before cloning into the bidirectional transfer vector downstream of the hPGK promoter, in place of the ΔLNGFR gene to create pCCL.sin_PPT.SV40polyA.GFP.minhCMV.hPGKHTTN-171Myc18Q.WPRE and pCCL.sin_PPT.SV40polyA.GFP.minhCMV.hPGKHTTN171Myc82Q.WPRE respectively. Codon optimized Human $VEGF_{165}$ (NCBI Ref. Seq. NP_001165097.1) and Hsp70 (NCBI Ref. Seq. NC_000005.9) incorporating a Kozak sequence to increase translational initiation and two stop codons to ensure efficient termination were synthesized by GENEart (Life Technologies, Paisley, UK). $VEGF_{165}$ or Hsp70 was subcloned into pCR2.1-TOPO to add additional restriction sites before cloning into final transfer vector downstream of hPGK. The red fluorescent protein from DsRed2-N1 (kind gift by Massimo Pizzato) was subcloned into pCR2.1-TOPO, then a shuttle vector p0.6(a) that carries the bidirectional promoter (kindly provided by Mario Amendola), before cloning into the final transfer vectors under the minhCMV promoter giving rise to pCCL.sin_PPT.SV40polyA.RFP.minhCMV.hPGK.h$VEGF_{165}$.WPRE and pCCL.sin_PPT.SV40polyA.RFP.minhCMV.hPGK.HSP70.WPRE. All constructs were verified by restriction enzyme digest and sequencing.

Protein analysis

Western blotting: To confirm transgene protein expression, 293T cells were transfected with each of the newly generated transfer plasmids using Lipofectamine LTX reagent (Invitrogen; 15338-100). Forty-eight hours after transfection, cell lysates were prepared by the addition of RIPA buffer plus inhibitor cocktail (Thermo, Loughborough, UK; 89908 and 78440) and protein levels assessed by the Bradford assay and normalized. Lysates were boiled in 1× Laemmli buffer (6×; 259 mmol/l Tris pH 6.8, 10% (w/v) SDS, 40% (v/v) glycerol, 0.6 µmol/l dithiothreitol) and run on a 10% SDS-PAGE gel. Separated proteins were transferred onto nitrocellulose membrane (Hybond-ECL, GE Healthcare, Chalfont St Giles, UK), blocked with PBS/Tween-20 (0.1% (v/v)) with 5% (w/v) milk powder) and probed with antibodies to $VEGF_{165}$ (Santa Cruz, Santa Cruz, CA; sc-7269) or HSP70 (Santa Cruz; sc-59569), c-Myc (tag HTT) (Santa Cruz; sc-56634) and GAPDH (Santa Cruz; sc-47724). Antibody-recognized proteins were detected using a horseradish peroxidase-conjugated anti-rabbit IgG secondary (Sigma) and ECL reagent (Pierce, Loughborough, UK).

ELISA: To confirm the presence of $VEGF_{165}$ in the supernatant of 293T cells transduced with $VEGF_{165}$ expressing LV vector (MOI 10), an ELISA was performed 72 hours after transduction against human VEGF according to the manufacturer's protocol (R&D Systems, Abingdon, UK; DVE00).

Production and purification of LVs. HIV-1–based LVs were produced using a standard transient calcium phosphate transfection protocol.[34] Briefly, 12 × 150 mm tissue culture dishes were seeded with 1.4×10^7 293T cells per dish. The following day cells were transfected with 32 µg of the relevant bicistronic transfer vector plasmid (expressing either eGFP or RFP reporter gene and huntingtin or $VEGF_{165}$ or Hsp70 or lacking a transgene), 12.5 µg plasmid expressing the HIV-1 gag/pol gene (pMD2-LgpRRE), 6.25 µg plasmid expressing HIV-1 Rev (pRSV-Rev), 9 µg of the VSVg envelope, and 15 µg pAdvantage plasmid to enhance viral production. Sixteen hours transfection, media was replaced with fresh media supplemented with 10 mmol/l sodium butyrate. Thirty-six hours after sodium butyrate induction, media containing vector was filtered through a 45 µm filter and centrifuged overnight (Beckman, High Wycombe, UK; F500 rotor, 6,000*g*). The viral vector pellet was resuspended on ice with cold PBS and repelleted by ultracentrifugation (Beckman; SW-32 Ti rotor, 68,500*g*, 1.5 hours). The pellet was then resuspended over several hours

in TSSM formulation buffer (20 mmol/l tromethamine, 100 mmol/l NaCl, 10 mg/ml sucrose, and 10 mg/ml mannitol). Vector preps were stored at −80 °C. LVs were tested for bacterial contamination by inoculating liquid broth with a 5 µl aliquot of vector and incubating at 37 °C while shaking for 21 days. LVs were also tested for mycoplasma (Lonza, Slough, UK; LT07-418) and endotoxin (Pierce; 88282) contamination using specific kits following manufacturer's protocols.

Titration of LVs. The functional titers of LVs carrying either eGFP or RFP reporter genes were determined by flow cytometry. Briefly, 293T cells were seeded in 12-well plates at a density of 5×10^5 cells per well. 16–24 hours after seeding, cells in a single well were quantified using a hemocytometer. Cells in the remaining wells were transduced for 6 hours with a serial dilution of the vector in the presence of 8 µg/ml polybrene. Seventy-two hours after transduction, the percentage of GFP +ve cells was evaluated by flow cytometry and TU/ml calculated (TU/ml = no. cells on day of transduction × proportion of positive cells × dilution factor). The number of physical lentiviral particles present in the viral vector stock was estimated using a HIV-1 p24 Antigen ELISA (RETROtek from ZeptoMetrix, Buffalo, NY).

Cell models of HD

SH-SY5Y transductions: Eight-well glass chambered slides were precoated with poly-D-lysine and laminin as follows: Four hundred microliter of 50 µg/ml poly-D-lysine (Sigma, P6407) was added to each well and slides were incubated for 2 hours at room temperature. Wells were washed three times with tissue culture H_2O and allowed to air dry before the addition of 400 µl of 10 µg/ml laminin (Sigma, L-2020). Laminin coated slides were incubated overnight at 37 °C and washed three times with phosphate buffered saline before seeding cells. SH-SY5Y cells were seeded at 80,000 cells per well, 16–20 hours after seeding cells were transduced with LVs at an MOI of 25 and after 6 hours the medium was refreshed. After 48 hours, half of the medium for each well was refreshed. Ninety-six hours after transduction, cell death, apoptosis, and aggregate formation were assessed. To evaluate the percentage cell death, all cells from each treatment were stained with trypan blue solution (0.4%; Sigma). The number of stained and unstained cells were quantified by hemocytometer count from $5 \times 1\,mm^2$ squares for each sample and the percentage cell death calculated. To quantify cells undergoing apoptosis, adherent cells were incubated with 5 µg/ml Hoechst 33342 (Sigma; B2261) for 15 minutes at 37 °C and then analyzed by fluorescent microscopy. Apoptotic cells were distinguished by bright blue staining. Images were captured at 40× magnification and the number of apoptotic cells quantified from 10 fields of view per sample.

Primary striatal neuron transductions: Primary rat striatal neurons were seeded at 1.2×10^5 cells per well in poly-D-lysine coated eight-well chambered slides. Striatal cultures were transduced at DIV 1 with LVs at an MOI of 10 and medium replaced with conditioned medium after 6 hours. Cultures were kept for 6 weeks, with a weekly medium change, and cell survival and aggregates assessed by NeuN and EM48 immunohistochemistry.

Stereotaxic surgery. All animal procedures were approved by the local Ethical Committee and performed in accordance with United Kingdom Animals Scientific Procedures Act (1986) and associated guidelines. All efforts were made to minimize the suffering and the number of animals used. Adult male wistar rats of 300–350 g were used for stereotaxic experiments. The animals were housed under a 12-hour light/dark cycle (light phase, 7:00 p.m. to 7:00 a.m.) with food and water available *ad libitum*. Animals were supplied by Harlan, Blackthorn, UK.

Before surgery, all animals were deeply anesthetized by inhalation of a mixture of 3L oxygen and 3.5% isoflurane (Merial, Harlow, UK) and then received systemic analgesia. They were placed in a stereotactic frame (Taxic-6000; World Precision Instruments, Sarasota, FL) with the nose bar at 3.3 mm. The anesthetic mixture was changed to 1L oxygen and 2.2% isoflurane for the remainder of the operation. The scalp was cut and retracted to expose the skull. Craniotomy was performed by drilling directly above the target region, to expose the pial surface. One single injection was directed into the right striatum using the stereotactic coordinates relative to bregma: anteroposterior, 0.5 mm; mediolateral, 3.0 mm; dorsoventral, 5.0 mm. Each rat received 6.0 µl of LV via a 32G blunt needle using an infusion pump (UltramicropumpIII and Micro4 Controller; World Precision Instruments) at a flow rate of 0.2 µl/minutes over 30 minutes. The needle was then allowed to remain on site for an additional 5 minutes before slow retraction. At the completion of surgery, the skin was sutured. For the lower VEGF$_{165}$ dose experiments, rats received 4 µl 82Q LV (1.25×10^9 TU/ml, 1.65×10^5 ng p24/ml) and either 1 µl VEGF LV (1.89×10^8 TU/ml, 5.21×10^4 ng p24/ml) or 0.5 µl of ΔLNGFR control (4×10^8 TU/ml, 1.64×10^5 ng/ml) and made up to a total injection volume of 6 µl with TSSM. For the higher dose VEGF experiments, rats received 3 µl 82Q LV (1.4×10^9 TU/ml, 2.94×10^5 ng p24/ml) and either 2.2 µl VEGF LV (8.8×10^8 TU/ml, 3.95×10^5 ng p24/ml) or 3 µl of RFP control (8.19×10^8 TU/ml, 1.33×10^5 ng/ml) and made up to a total injection volume of 6 µl with TSSM.

Rats were euthanized 10 weeks after injection by intraperitoneal injection of an overdose of sodium pentobarbitone, transcardially perfused with 50 ml ice-cold saline (0.9% w/v NaCl) plus heparin (20 U/ml), followed by 250 ml of 4% paraformaldehyde (Sigma). Brains were removed and post-fixed for 4 hours in 4% paraformaldehyde, followed by cryoprotection in 10% glycerol and 20% sucrose in 1× PBS for at least 72 hours. Brains were subsequently embedded and frozen in OCT (Surgipath FSC22; Leica Microsystems, Wetzlar, Germany). Thirty micron coronal sections from the entire striatum were cut using a cryostat (Leica Microsystems), mounted on poly-L-lysine coated slides and stored at −20 °C.

Immunohistochemistry

Immunostaining of cell cultures: To evaluate the neuronal cell and aggregate numbers, cells were fixed for 15 minutes at room temperature with 4% paraformaldehyde in PBS. After washing for 5 minutes with PBS, cells were permeabilized for 30 minutes in permeabilization buffer (10% goat serum, TBS, 0.5% triton X-100), washed again and incubated with normal blocking serum (Vectastain ABC kit, PK-6200; Vector Labs, Peterborough, UK) for 20 minutes. Cells were then incubated at 4 °C overnight with either mouse anti-NeuN (Millipore; MAB377) or mouse anti-huntingtin protein monoclonal antibody (clone mEM48; Millipore, Watford, UK; MAB5374). After washing, the secondary antibody (biotinylated antibody; Vectastain ABC kit) was applied, and color was developed using the Vectastain ABC reagent and DAB (Vectastain ABC kit). Immunostaining was examined under Nikon Eclipse TS100 inverted system microscope.

Immunostaining of brain sections: Free floating brain sections were permeabilized and blocked for 1 hour in permeabilization buffer. Antibodies were prepared in blocking buffer (10% goat serum, TBS, 0.03% triton X-100) to the following working dilutions: eGFP (1:500; Abcam, Cambridge, UK; ab290), NeuN (1:200; Millipore; MAB377), DARRP32 (1:1,000; Abcam; ab40801), EM48 (1:400; Millipore; MAB5374), 2B4 (1:200; Millipore; MAB5492), ubiquitin (1:200, Dako Z0458), Glut-1 (1:250; Abcam; ab652), albumin (1:400, MPI cappel 55728), c-Myc (1:100; Santa Cruz; sc-56634), ED1 (1:200; Abcam; ab31630), CD4 (1:200; Abcam; ab33775) and CD8 (1:200; Abcam; ab33786). Sections were incubated in primary antibody for 48 hours, washed three times with TBS and incubated in blocking buffer for 30 minutes before incubation with goat anti-mouse or anti-rabbit secondary antibodies conjugated with alexa fluor 488 or 594 (1:400, Invitrogen) for 2 hours at RT. Sections were then washed five times with TBS before being mounted with polyvinyl alcohol mounting medium with DABCO anti-fade (Sigma, 10981) in presence of 0.05 µg/ml DAPI (Lonza) to label nuclear DNA.

Image analysis and counting. Images from fluorescent–labeled sections (striatum) were taken under an epifluorescent microscope (Eclipse 80i; Nikon, Tokyo, Japan) equipped with a motorized stage for automated tiling of adjacent fields (Prior Scientific, Cambridge, UK). For DARPP-32

depletion assessment, a series of sections throughout the striatum 180 μm apart (caudate and putamen) were used for immunostaining. Images were captured at 4× magnification. The area of DARPP-32 depletion in mm^2 for each section was calculated with a computer-assisted imaging program (Image Pro Plus 7.0; Media Cybernetics, Rockville, MD). Lesion areas in each section were determined as region poor in DARPP-32 staining relative to the surrounding area. The total volume DARPP-32 depletion was estimated using the following equation: volume = $d(a_1 + a_2 + a_3 \ldots)$, where d is the distance between sections (180 μm), and $a_1, a_2, a_3 \ldots$ are DARPP-32-depleted areas for individual sections. For huntingtin aggregate counts, five fields of view were captured for each section at 4× magnification and then image analysis software (Image Pro Plus 7.0) was used to count aggregates at a defined threshold intensity. The aggregate count for each animal was determined and then averaged for each group.

Bioinformatics and statistics. The amino acid sequences for transfer vector plasmids were aligned using DNA dynamo software. Statistics were analyzed and graphed using GraphPad Prism software (Graphpad Software, La Jolla, CA). Data are expressed as mean ± SEM and were evaluated by either one-way analysis of variance or paired Student's *t*-test.

SUPPLEMENTARY MATERIAL

Figure S1. LV HD *in vivo* model.
Figure S2. VEGF overexpression in wild-type striatum induces overt toxicity, vascularization and death.
Figure S3. VEGF overexpression in wild-type striatum induces extensive macrophage/monocyte infiltration.

ACKNOWLEDGMENTS

We thank Mario Amendola and Professor Luigi Naldini (Vita-Salute San Raffaele University Medical School, Milan, Italy) for bidirectional transfer vectors; Nicole Deglon (Atomic Energy Commission (CEA) Orsey France) for huntingtin sequences; Professor RI Morimoto (NorthWestern University, Evaston, USA) for Hsp70 cDNA clone pC-MVHsp70; pDsRed2 was a kind gift from Massimo Pizzato (Imperial College London); Louis de Almeida (University of Coimbra Portugal) for advice on DARRP32 immunohistochemistry; Professor Richard Reynolds (Imperial College London) for use of confocal microscope and critical reading of this manuscript; and Zelie Britton (Imperial College Medical School student) for technical assistance. This work was funded from a grant from HighQ/CHDI foundation to N.D.M. supporting V.T., S.M.T., and A.T. are supported by an advanced investigators ERC grant awarded to N.D.M., E.P., S.L., V.P., D.G., S.M., and N.M. were master degree students in the N.D.M. lab that were supported by Imperial College funds. The authors declared no conflict of interest.

REFERENCES

1. A novel gene containing a trinucleotide repeat that is expanded and unstable on Huntington's disease chromosomes. The Huntington's Disease Collaborative Research Group. *Cell* **72**: 971–983 (1993).
2. Vonsattel, JP and DiFiglia, M (1998). Huntington disease. *J Neuropathol Exp Neurol* **57**: 369–384.
3. Roze, E, Cahill, E, Martin, E, Bonnet, C, Vanhoutte, P, Betuing, S *et al.* (2011). Huntington's Disease and Striatal Signaling. *Front Neuroanat* **5**: 55.
4. Almeida, MB, do Nascimento, JL, Herculano, AM and Crespo-López, ME (2011). Molecular chaperones: toward new therapeutic tools. *Biomed Pharmacother* **65**: 239–243.
5. Satyal, SH, Schmidt, E, Kitagawa, K, Sondheimer, N, Lindquist, S, Kramer, JM *et al.* (2000). Polyglutamine aggregates alter protein folding homeostasis in Caenorhabditis elegans. *Proc Natl Acad Sci USA* **97**: 5750–5755.
6. Perrin, V, Régulier, E, Abbas-Terki, T, Hassig, R, Brouillet, E, Aebischer, P *et al.* (2007). Neuroprotection by Hsp104 and Hsp27 in lentiviral-based rat models of Huntington's disease. *Mol Ther* **15**: 903–911.
7. Krobitsch, S and Lindquist, S (2000). Aggregation of huntingtin in yeast varies with the length of the polyglutamine expansion and the expression of chaperone proteins. *Proc Natl Acad Sci USA* **97**: 1589–1594.
8. Jana, NR, Tanaka, M, Wang, Gh and Nukina, N (2000). Polyglutamine length-dependent interaction of Hsp40 and Hsp70 family chaperones with truncated N-terminal huntingtin: their role in suppression of aggregation and cellular toxicity. *Hum Mol Genet* **9**: 2009–2018.
9. Chan, HY, Warrick, JM, Gray-Board, GL, Paulson, HL and Bonini, NM (2000). Mechanisms of chaperone suppression of polyglutamine disease: selectivity, synergy and modulation of protein solubility in Drosophila. *Hum Mol Genet* **9**: 2811–2820.
10. McBride, JL, During, MJ, Wuu, J, Chen, EY, Leurgans, SE and Kordower, JH (2003). Structural and functional neuroprotection in a rat model of Huntington's disease by viral gene transfer of GDNF. *Exp Neurol* **181**: 213–223.
11. Kells, AP, Fong, DM, Dragunow, M, During, MJ, Young, D and Connor, B (2004). AAV-mediated gene delivery of BDNF or GDNF is neuroprotective in a model of Huntington disease. *Mol Ther* **9**: 682–688.
12. Giralt, A, Friedman, HC, Caneda-Ferrón, B, Urbán, N, Moreno, E, Rubio, N *et al.* (2010). BDNF regulation under GFAP promoter provides engineered astrocytes as a new approach for long-term protection in Huntington's disease. *Gene Ther* **17**: 1294–1308.
13. Gharami, K, Xie, Y, An, JJ, Tonegawa, S and Xu, B (2008). Brain-derived neurotrophic factor over-expression in the forebrain ameliorates Huntington's disease phenotypes in mice. *J Neurochem* **105**: 369–379.
14. de Almeida, LP, Zala, D, Aebischer, P and Déglon, N (2001). Neuroprotective effect of a CNTF-expressing lentiviral vector in the quinolinic acid rat model of Huntington's disease. *Neurobiol Dis* **8**: 433–446.
15. Senger, DR, Galli, SJ, Dvorak, AM, Perruzzi, CA, Harvey, VS and Dvorak, HF (1983). Tumor cells secrete a vascular permeability factor that promotes accumulation of ascites fluid. *Science* **219**: 983–985.
16. Ferrara, N and Henzel, WJ (1989). Pituitary follicular cells secrete a novel heparin-binding growth factor specific for vascular endothelial cells. *Biochem Biophys Res Commun* **161**: 851–858.
17. Dvorak, HF (2002). Vascular permeability factor/vascular endothelial growth factor: a critical cytokine in tumor angiogenesis and a potential target for diagnosis and therapy. *J Clin Oncol* **20**: 4368–4380.
18. Oosthuyse, B, Moons, L, Storkebaum, E, Beck, H, Nuyens, D, Brusselmans, K *et al.* (2001). Deletion of the hypoxia-response element in the vascular endothelial growth factor promoter causes motor neuron degeneration. *Nat Genet* **28**: 131–138.
19. Azzouz, M, Ralph, GS, Storkebaum, E, Walmsley, LE, Mitrophanous, KA, Kingsman, SM *et al.* (2004). VEGF delivery with retrogradely transported lentivector prolongs survival in a mouse ALS model. *Nature* **429**: 413–417.
20. Storkebaum, E, Lambrechts, D, Dewerchin, M, Moreno-Murciano, MP, Appelmans, S, Oh, H *et al.* (2005). Treatment of motoneuron degeneration by intracerebroventricular delivery of VEGF in a rat model of ALS. *Nat Neurosci* **8**: 85–92.
21. Lunn, JS, Sakowski, SA, Kim, B, Rosenberg, AA and Feldman, EL (2009). Vascular endothelial growth factor prevents G93A-SOD1-induced motor neuron degeneration. *Dev Neurobiol* **69**: 871–884.
22. Azzouz, M, Kingsman, SM and Mazarakis, ND (2004). Lentiviral vectors for treating and modeling human CNS disorders. *J Gene Med* **6**: 951–962.
23. Zala, D, Benchoua, A, Brouillet, E, Perrin, V, Gaillard, MC, Zurn, AD *et al.* (2005). Progressive and selective striatal degeneration in primary neuronal cultures using lentiviral vector coding for a mutant huntingtin fragment. *Neurobiol Dis* **20**: 785–798.
24. Palfi, S, Brouillet, E, Jarraya, B, Bloch, J, Jan, C, Shin, M *et al.* (2007). Expression of mutated huntingtin fragment in the putamen is sufficient to produce abnormal movement in non-human primates. *Mol Ther* **15**: 1444–1451.
25. de Almeida, LP, Ross, CA, Zala, D, Aebischer, P and Déglon, N (2002). Lentiviral-mediated delivery of mutant huntingtin in the striatum of rats induces a selective neuropathology modulated by polyglutamine repeat size, huntingtin expression levels, and protein length. *J Neurosci* **22**: 3473–3483.
26. Martin, E, Betuing, S, Pagès, C, Cambon, K, Auregan, G, Deglon, N *et al.* (2011). Mitogen- and stress-activated protein kinase 1-induced neuroprotection in Huntington's disease: role on chromatin remodeling at the PGC-1-alpha promoter. *Hum Mol Genet* **20**: 2422–2434.
27. Amendola, M, Venneri, MA, Biffi, A, Vigna, E and Naldini, L (2005). Coordinate dual-gene transgenesis by lentiviral vectors carrying synthetic bidirectional promoters. *Nat Biotechnol* **23**: 108–116.
28. Wyttenbach, A, Carmichael, J, Swartz, J, Furlong, RA, Narain, Y, Rankin, J *et al.* (2000). Effects of heat shock, heat shock protein 40 (HDJ-2), and proteasome inhibition on protein aggregation in cellular models of Huntington's disease. *Proc Natl Acad Sci USA* **97**: 2898–2903.
29. Simpson, CS, Johnston, HM and Morris, BJ (1994). Phenotypic characterisation of rat striatal neurones in primary culture. *Tissue Cell* **26**: 929–941.
30. Régulier, E, Trottier, Y, Perrin, V, Aebischer, P and Déglon, N (2003). Early and reversible neuropathology induced by tetracycline-regulated lentiviral overexpression of mutant huntingtin in rat striatum. *Hum Mol Genet* **12**: 2827–2836.
31. Xiong, N, Zhang, Z, Huang, J, Chen, C, Zhang, Z, Jia, M *et al.* (2011). VEGF-expressing human umbilical cord mesenchymal stem cells, an improved therapy strategy for Parkinson's disease. *Gene Ther* **18**: 394–402.
32. Mani, N, Khaibullina, A, Krum, JM and Rosenstein, JM (2005). Astrocyte growth effects of vascular endothelial growth factor (VEGF) application to perinatal neocortical explants: receptor mediation and signal transduction pathways. *Exp Neurol* **192**: 394–406.
33. Greenberg, DA and Jin, K (2005). From angiogenesis to neuropathology. *Nature* **438**: 954–959.
34. Yeh, WL, Lin, CJ and Fu, WM (2008). Enhancement of glucose transporter expression of brain endothelial cells by vascular endothelial growth factor derived from glioma exposed to hypoxia. *Mol Pharmacol* **73**: 170–177.
35. Krum, JM, Mani, N and Rosenstein, JM (2002). Angiogenic and astroglial responses to vascular endothelial growth factor administration in adult rat brain. *Neuroscience* **110**: 589–604.
36. Sofroniew, MV (2005). Reactive astrocytes in neural repair and protection. *Neuroscientist* **11**: 400–407.
37. Clauss, M, Gerlach, M, Gerlach, H, Brett, J, Wang, F, Familletti, PC *et al.* (1990). Vascular permeability factor: a tumor-derived polypeptide that induces endothelial cell and monocyte procoagulant activity, and promotes monocyte migration. *J Exp Med* **172**: 1535–1545.
38. Storkebaum, E, Lambrechts, D and Carmeliet, P (2004). VEGF: once regarded as a specific angiogenic factor, now implicated in neuroprotection. *Bioessays* **26**: 943–954.

39. Matsuzaki, H, Tamatani, M, Yamaguchi, A, Namikawa, K, Kiyama, H, Vitek, MP *et al.* (2001). Vascular endothelial growth factor rescues hippocampal neurons from glutamate-induced toxicity: signal transduction cascades. *FASEB J* **15**: 1218–1220.
40. Van Den Bosch, L, Storkebaum, E, Vleminckx, V, Moons, L, Vanopdenbosch, L, Scheveneels, W *et al.* (2004). Effects of vascular endothelial growth factor (VEGF) on motor neuron degeneration. *Neurobiol Dis* **17**: 21–28.
41. Svensson, B, Peters, M, König, HG, Poppe, M, Levkau, B, Rothermundt, M *et al.* (2002). Vascular endothelial growth factor protects cultured rat hippocampal neurons against hypoxic injury via an antiexcitotoxic, caspase-independent mechanism. *J Cereb Blood Flow Metab* **22**: 1170–1175.
42. Silverman, WF, Krum, JM, Mani, N and Rosenstein, JM (1999). Vascular, glial and neuronal effects of vascular endothelial growth factor in mesencephalic explant cultures. *Neuroscience* **90**: 1529–1541.
43. Ogunshola, OO, Antic, A, Donoghue, MJ, Fan, SY, Kim, H, Stewart, WB *et al.* (2002). Paracrine and autocrine functions of neuronal vascular endothelial growth factor (VEGF) in the central nervous system. *J Biol Chem* **277**: 11410–11415.
44. Jin, K, Mao, XO, Batteur, SP, McEachron, E, Leahy, A and Greenberg, DA (2001). Caspase-3 and the regulation of hypoxic neuronal death by vascular endothelial growth factor. *Neuroscience* **108**: 351–358.
45. Wang, Y, Mao, XO, Xie, L, Banwait, S, Marti, HH, Greenberg, DA *et al.* (2007). Vascular endothelial growth factor overexpression delays neurodegeneration and prolongs survival in amyotrophic lateral sclerosis mice. *J Neurosci* **27**: 304–307.
46. Tian, YY, Tang, CJ, Wang, JN, Feng, Y, Chen, XW, Wang, L *et al.* (2007). Favorable effects of VEGF gene transfer on a rat model of Parkinson disease using adeno-associated viral vectors. *Neurosci Lett* **421**: 239–244.
47. Emerich, DF, Mooney, DJ, Storrie, H, Babu, RS and Kordower, JH (2010). Injectable hydrogels providing sustained delivery of vascular endothelial growth factor are neuroprotective in a rat model of Huntington's disease. *Neurotox Res* **17**: 66–74.
48. Zala, D, Bensadoun, JC, Pereira de Almeida, L, Leavitt, BR, Gutekunst, CA, Aebischer, P *et al.* (2004). Long-term lentiviral-mediated expression of ciliary neurotrophic factor in the striatum of Huntington's disease transgenic mice. *Exp Neurol* **185**: 26–35.
49. Proescholdt, MA, Heiss, JD, Walbridge, S, Mühlhauser, J, Capogrossi, MC, Oldfield, EH *et al.* (1999). Vascular endothelial growth factor (VEGF) modulates vascular permeability and inflammation in rat brain. *J Neuropathol Exp Neurol* **58**: 613–627.
50. Argaw, AT, Asp, L, Zhang, J, Navrazhina, K, Pham, T, Mariani, JN *et al.* (2012). Astrocyte-derived VEGF-A drives blood-brain barrier disruption in CNS inflammatory disease. *J Clin Invest* **122**: 2454–2468.